

Ab initio calculation of the potential energy surface for the dissociation of H₂ on the sulfur covered Pd(100) surface

C. M. Wei*, A. Groß, and M. Scheffler
*Fritz-Haber-Institut der Max-Planck-Gesellschaft,
Faradayweg 4-6, D-14 195 Berlin-Dahlem, Germany*

The presence of sulfur atoms on the Pd(100) surface is known to hinder the dissociative adsorption of hydrogen. Using density-functional theory and the full-potential linear augmented plane-wave method, we investigate the potential energy surface (PES) of the dissociative adsorption of H₂ on the sulfur covered Pd(100) surface. The PES is changed significantly compared to the dissociation on the clean Pd(100) surface, in particular for hydrogen close to the S atoms. While the hydrogen dissociation at the clean Pd(100) surface is non-activated, for the (2×2) sulfur adlayer (coverage $\Theta_S = 0.25$) the dissociation of H₂ is inhibited by energy barriers. Their heights strongly depend on the distance between the hydrogen and sulfur atoms leading to a highly corrugated PES. The largest barriers are in the vicinity of the sulfur atoms due to the strong repulsion between sulfur and hydrogen. Still the hydrogen dissociation on the (2×2) sulfur covered Pd(100) surface is exothermic. Thus the poisoning effect of sulfur adatoms for H₂ dissociation at low sulfur coverage ($\Theta_S \leq 0.25$) is mainly governed by the formation of energy barriers, not by blocking of the adsorption sites. For the c(2×2) sulfur adlayer ($\Theta_S = 0.5$), the PES for hydrogen dissociation is purely repulsive. This is due to the fact that for all different possible adsorption geometries the hydrogen molecules come too close to the sulfur adatoms before the dissociation is completed.

PACS numbers: 68.45.Da, 73.20.At, 82.65.Jv

I. INTRODUCTION

The modification of the chemical reactivity and selectivity of surfaces by adsorbates is important for, e.g., building better catalysts. Therefore the investigation of the microscopic mechanisms of how adatoms poison or promote certain reactions is – besides its fundamental interest – of great technological relevance. Hydrogen dissociation has become the benchmark system for theoretical and experimental studies of simple chemical reactions on surfaces. On clean metal surfaces, a detailed picture of how H-H bonds are broken and how new bonds between the hydrogen atoms and the surface are formed has been developed by theoretical studies.^{1–9} The modification of the potential energy surface (PES) of hydrogen dissociation on an adlayer-covered surface has not been addressed in similar detail by theory so far.

Experimentally it is well established that the presence of sulfur on metal surfaces causes a drastic reduction in hydrogen sticking probabilities.^{10–13} Earlier theoret-

ical studies explaining the poisoning mechanism focused on general concepts. Feibelman and Hamann^{14,15} suggested that the poisoning effect of sulfur is related to the sulfur induced change of the density of states (DOS) at the Fermi level. This explanation was also employed by MacLaren and co-workers.¹⁶ Current studies, however, have emphasized that the reactivity of surfaces cannot be solely understood by the DOS at the Fermi level.^{17,18} A different model for the poisoning was proposed by Nørskov *et al.*^{19–21} These authors explain the modification of the reactivity by adlayers by the interaction of the H₂ molecule with the adlayer induced electrostatic field. These models, however, do not provide a detailed microscopic picture of how the hydrogen dissociation process is actually modified by the adlayer, i.e., either by blocking adsorption sites for atomic hydrogen or by building up energy barriers along the dissociation pathways of H₂.

Recently the poisoning mechanism of Pd(100) by a sulfur adlayer has been investigated theoretically by Wilke and Scheffler.^{22,23} The Pd(100) surface is a well-suited substrate for the investigation of the poisoning mechanism of catalytic reactions, because many experimental and theoretical studies exist and form a wealth of information for comparison. At the clean surface, hydrogen molecules dissociate spontaneously, i.e., non-activated dissociation pathways exist with no hampering energy barrier.^{8,12,13,24,25} When the surface is covered with sulfur, the H₂ sticking probability is significantly reduced.^{12,13} These experiments show that with increasing sulfur coverages Θ_S the initial sticking coefficient of H₂ strongly decreases. This is true in particular for molecules with low kinetic energy¹² (≤ 0.1 eV) that can adsorb only if nonactivated dissociation pathways exist and are accessible. For $\Theta_S \approx 0.25$ the initial sticking coefficient of molecules with low energies is approximately two orders of magnitude smaller than the one for the clean surface,^{12,13} indicating that for this sulfur coverage non-activated dissociation is nearly completely hindered. When the sulfur coverage is increased, the initial sticking coefficient reduces even further; at $\Theta_S \approx 0.5$ it is about three orders of smaller than at the clean surface.¹² In addition to the significant decrease of the initial sticking coefficient, TPD studies¹³ observed a decrease of the hydrogen saturation coverage with increasing Θ_S . Burke and Madix¹³ therefore concluded that sulfur adatoms substantially reduce the hydrogen adsorption energy at sites in their vicinity, making these positions unstable against associative desorption. An earlier permeation study of Comsa, David, and Schumacher²⁴ led to the same con-

clusion.

These findings are at variance with the results of Wilke and Scheffler.^{22,23} They showed by density-functional theory calculations that the hydrogen dissociation at the (2×2) sulfur covered Pd(100) surface is still exothermic and that the blocking of adsorption sites is therefore only of minor importance at low coverages. Adsorbed sulfur builds up energy barriers in the entrance channel and thus hinders the dissociation. Their results gave a clear explanation for the poisoning mechanism. We have now extended their work. We have investigated in detail how the poisoning of the hydrogen dissociation on Pd(100) by the presence of sulfur depends on the position and orientation of the molecule. Furthermore, we have addressed the influence of the sulfur coverage on the poisoning.

In this paper, using density-functional theory and the full-potential linear augmented plane wave (FLAPW) method, we calculate the PES of H₂ dissociative adsorption over the (2×2) and the c(2×2) sulfur covered Pd(100) surface at different adsorption sites and different orientations, and thus provide a complete picture of the poisoning mechanism caused by the adsorbed sulfur on Pd(100) surface. We fully confirm the conclusions of Wilke and Scheffler^{22,23}: the poisoning effect of sulfur adatoms for H₂ dissociation over Pd(100) surface at low sulfur coverage ($\Theta_S \leq 0.25$) is governed by the formation of energy barriers. The height of the energy barriers depends strongly on the distance between H₂ and the S atoms. For high sulfur coverage ($\Theta_S = 0.5$), the PES for hydrogen dissociation becomes purely repulsive due to the fact that for all possible different adsorption geometries the hydrogen molecules come too close to the sulfur adatoms before the dissociation is completed. The results are now sufficiently complete for a six-dimensional quantum dynamical simulation²⁶. This requires the representation of the *ab initio* PES by an analytical function²⁷ in order to interpolate the actually calculated points and to achieve a closed expression of the PES. This will be also presented in this paper.

The structure of the paper is as follows. In Section II we describe the theoretical method and computational details. The potential energy surface for the hydrogen dissociation on the (2×2) sulfur covered Pd(100) surface at different adsorption sites is presented and discussed in Section III. Section IV reports the results of the H₂ interaction with the c(2×2) sulfur covered Pd(100) surface. The dependence of the PES on the orientation of the molecule is analysed in Section V. After a brief description of the analytical representation of the PES suitable for a quantum dynamical simulation in Section VI, the paper concludes with a summary in Section VII.

II. COMPUTATIONAL DETAILS

We have used density-functional theory together with the generalized gradient approximation (GGA)²⁸ for the

exchange-correlation functional. The full-potential linear augmented plane wave (FLAPW) method^{29,30} is employed for solving the non-relativistic Kohn-Sham equations. The FLAPW wave functions in the interstitial region are represented using a plane wave expansion up to $E_{\text{cut}} = 11$ Ry. For the potential representation plane waves up to $E_{\text{cut}} = 169$ Ry are taken into account due to a small muffin-tin radius around the H atoms ($r_{MT}^H = 0.37$ Å). Inside the muffin-tin spheres the wave functions are expanded in spherical harmonics with $l_{\text{max}} = 10$, and non-spherical components of the density and potential are included up to $l_{\text{max}} = 4$. For the \mathbf{k} -space integration, a grid of 5×5 (or 6×6) uniformly spaced points are used in the two-dimensional Brillouin zone of the (2×2) [or the c(2×2)] surface unit cell, and we find that for a finer mesh the adsorption energies change by at most 30 meV for the (2×2) hollow site adsorption geometry.

We used a supercell geometry and modeled the metal surface by three-layer slabs which were separated by a 12 Å vacuum region. Hydrogen and sulfur atoms were placed at both sides of the slab. For the geometry of the sulfur covered Pd(100) surface, the results reported in Ref. 22 were used. Tests were made for a five-layer slab at different adsorption geometries, and the average total energy difference from a three-layer slab calculation was found to be less than 40 meV (see Table I). This agrees with results reported by Wilke and Scheffler²³ who also studied the influence of the slab thickness on the potential energy for slabs with up to seven layers. They found energy differences of less than 30 meV for the barrier heights and the adsorption energies at the hollow sites of the surface.

The substrate geometry was kept fixed for the H₂ adsorption pathways studied. This is appropriate and plausible because the mass mismatch of H with the substrate atoms is significant. The energy zero is taken as the energy of the geometry where the molecule is sufficiently far away from the surface ($Z = 4.03$ Å) such that there is practically no interaction between the molecule and the surface. Zero-point corrections are not included in the PES.

III. H₂ AT THE (2×2) SULFUR COVERED Pd(100) SURFACE

A. Determination of the potential energy surface (PES)

Neglecting surface relaxation effects, the potential energy surface for the dissociative adsorption of a hydrogen molecule over a sulfur covered Pd(100) surface is six-dimensional corresponding to the molecular degrees of freedom. The coordinates used in this work are defined in Fig. 1. The H₂ center of mass position is given by three Cartesian coordinates (X, Y, Z) for which the origin is chosen as the hollow position of the topmost Pd layer.

The two rotational degrees of freedom are given by the angle θ of the molecular axis with the Z -axis (cartwheel rotation) and the angle ϕ with the X -axis (helicopter rotation). The distance between the hydrogen atoms is denoted by $d_{\text{H-H}}$.

To map this high-dimensional energy surface the common strategy is to compute two-dimensional cuts through the energy surface, so-called elbow-plots, where (X, Y, θ, ϕ) are fixed, and only $d_{\text{H-H}}$ (the bond length of the hydrogen molecule) and Z (its height above the surface) are varied. Figure 2 shows the surface unit cell for the (2×2) sulfur covered Pd(100) surface. Inside the unit cell, there are two bridge sites \mathbf{b}_1 and \mathbf{b}_2 , two hollow sites \mathbf{h}_1 and \mathbf{h}_2 , the top site above the Pd atom \mathbf{t}_{Pd} , and the top site above the S atom \mathbf{t}_{S} . In order to obtain a comprehensive information about the adsorption behavior of H_2 , we have evaluated the elbow-plots at different cuts through the six-dimensional configuration space of H_2 where the cuts are defined by the site (X, Y) and the molecular orientation (θ, ϕ) .

B. Results

To distinguish between the different molecular geometries, we characterize them by the set of fixed coordinates (X, Y, θ, ϕ) . For example, if one defines a as the unit length of the (2×2) unit cell, then $(0.5a, 0.5a, 0^\circ, 0^\circ)$ refers to a geometry with the hydrogen molecule placed at the \mathbf{h}_1 site in an upright position (molecular axis perpendicular to the surface); and $(0.5a, 0.5a, 90^\circ, \phi)$ refers to a geometry with the molecule at the \mathbf{h}_1 site with its axis parallel to surface. The geometry in which the molecule is parallel to the surface can also be characterized by the positions where the hydrogen atoms will be adsorbed, and by that over which the center of mass of the molecule is situated. For example $(0.5a, 0.25a, 90^\circ, 90^\circ)$ can be denoted by $\mathbf{h}_1\text{-}\mathbf{b}_1\text{-}\mathbf{h}_2$ which refers to a geometry with the center of mass over the bridge (\mathbf{b}_1) position and the atoms oriented towards the two hollow sites \mathbf{h}_1 and \mathbf{h}_2 in which they will finally be adsorbed.

1. 2-D cuts through the PES at hollow sites

For the PES of the hydrogen dissociation over the (2×2) S covered Pd(100) surface ($\Theta_{\text{S}} = 0.25$), two adsorption geometries $\mathbf{b}_1\text{-}\mathbf{h}_1\text{-}\mathbf{b}_1$ and $\mathbf{b}_1\text{-}\mathbf{h}_2\text{-}\mathbf{b}_1$ have been reported by Wilke and Scheffler.²³ Their results show that the presence of a the (2×2) S adlayer on Pd(100) changes the dissociation process significantly from being non-activated at the clean Pd(100) surface to activated dissociation. In their calculations, the dissociation pathways corresponding to the $\mathbf{b}_1\text{-}\mathbf{h}_1\text{-}\mathbf{b}_1$ and $\mathbf{b}_1\text{-}\mathbf{h}_2\text{-}\mathbf{b}_1$ geometries at the (2×2) sulfur covered Pd(100) surface had energy barriers in the entrance channel of 0.1 and 0.6 eV, respectively.

Figure 3(a) shows the re-calculated PES for the $\mathbf{b}_1\text{-}\mathbf{h}_1\text{-}\mathbf{b}_1$ adsorption geometry. The dissociation pathway has an energy barrier of 0.11 eV in the entrance channel which is consistent with previous calculations.²³ This configuration corresponds to the minimum barrier dissociation pathway. We will show below that the energy barriers increase as a function of decreasing distance of the hydrogen molecule to the sulfur atoms on the surface. For that reason it is not surprising that the $\mathbf{b}_1\text{-}\mathbf{h}_1\text{-}\mathbf{b}_1$ adsorption pathway exhibits the lowest energy barrier because the \mathbf{h}_1 hollow site is the site on the surface furthest away from the sulfur atoms.

Figure 3(b) shows the PES of the $\mathbf{t}_{\text{Pd}}\text{-}\mathbf{h}_1\text{-}\mathbf{t}_{\text{Pd}}$ pathway. At the clean Pd(100) surface, this path has a local minimum potential energy of -0.23 eV.³¹ The calculated results show that upon the adsorption of a (2×2) S adlayer an activation energy barrier towards dissociative adsorption of 0.13 eV builds up in the entrance channel at $(Z, d_{\text{H-H}}) = (1.7 \text{ \AA}, 0.78 \text{ \AA})$, and the minimum at $(Z, d_{\text{H-H}}) = (0.98 \text{ \AA}, 0.94 \text{ \AA})$ becomes very shallow with an energy of 0.01 eV. For this geometry, the two hydrogen atoms are about 3.3 \AA away from the adsorbed sulfur atoms, hence one can expect that there is no direct interaction between H and S atoms. In such a situation the energy increase is due to the sulfur-induced modification of the local electronic structure at the surface Pd atom²³, as will be confirmed below.

Figure 3(c) shows the PES for the $\mathbf{b}_2\text{-}\mathbf{h}_2\text{-}\mathbf{b}_2$ pathway. In this geometry the dissociation process becomes purely repulsive; it differs from the behavior at the $\mathbf{b}_1\text{-}\mathbf{h}_2\text{-}\mathbf{b}_1$ geometry where activated dissociation with an energy barrier of 0.6 eV is possible.²³ This is easy to understand because the hydrogen molecule dissociates towards the sulfur atoms at the $\mathbf{b}_2\text{-}\mathbf{h}_2\text{-}\mathbf{b}_2$ geometry, and the direct interaction between H and S atoms causes the dissociation process to become purely repulsive.

Figure 3(d) shows the PES for a geometry with the hydrogen molecule adsorbed at the \mathbf{h}_1 site in an upright position, i.e. with its molecular axis perpendicular to the surface. At the clean surface, there exists a shallow local minimum of -0.03 eV at $(Z, d_{\text{H-H}}) = (0.60 \text{ \AA}, 0.96 \text{ \AA})$.³¹ As is evident from Fig. 3(c), this pathway becomes repulsive upon the adsorption of the (2×2) S adlayer and the energy at $(Z, d_{\text{H-H}}) = (0.60 \text{ \AA}, 0.96 \text{ \AA})$ has raised to 0.28 eV from -0.03 eV. There is still a shallow well, however. For this geometry, the two hydrogen atoms directly above the \mathbf{h}_1 site are at least 4 \AA away from the adsorbed sulfur atoms, so there is no direct interaction between H and S atoms. Thus the increase in the potential energy has to be due to the sulfur-induced modification of the local electronic structure at this site.

2. 2-D cuts through the PES at bridge sites

In addition to the dissociation over the \mathbf{h}_1 and \mathbf{h}_2 hollow sites, we also considered geometries where the center

of mass of molecule is situated at the bridge site and the top sites over the Pd or S atoms. In Figures 4(a) and 4(b), the PES for the $\mathbf{h}_1\text{-}\mathbf{b}_1\text{-}\mathbf{h}_2$ and $\mathbf{t}_{\text{Pd}}\text{-}\mathbf{b}_1\text{-}\mathbf{t}_{\text{Pd}}$ pathways are presented.

At the clean surface, the dissociation pathway for $\mathbf{h}_1\text{-}\mathbf{b}_1\text{-}\mathbf{h}_2$ is non-activated. In Fig. 4(a), the PES for $\mathbf{h}_1\text{-}\mathbf{b}_1\text{-}\mathbf{h}_2$ geometry indicates that the adsorption of H_2 becomes an activated process with an energy barrier of 0.16 eV in the entrance channel ($Z=1.8 \text{ \AA}$ and $d_{\text{H-H}}=0.78 \text{ \AA}$). This energy barrier also results from the modification of the local electronic structure.²³ There exists a second barrier of 0.13 eV in the exit channel at $(Z, d_{\text{H-H}})=(0.97 \text{ \AA}, 1.05 \text{ \AA})$. We believe that this barrier might be due to the compensation between the direct attractive interaction of the Pd atoms with one H atom and the direct repulsive interaction of the S atoms with the other H atom, since the top of the energy barrier is situated at the value of Z close the sulfur adsorption height (1.24 \AA).

Figure 4(b) shows the PES for the $\mathbf{t}_{\text{Pd}}\text{-}\mathbf{b}_1\text{-}\mathbf{t}_{\text{Pd}}$ geometry. At the clean surface this dissociation pathway has a local energy minimum of -0.2 eV before becoming repulsive. Our calculations show that, upon adsorption of the S adlayer, the dissociation process becomes purely repulsive and is different from the behavior at the $\mathbf{h}_1\text{-}\mathbf{b}_1\text{-}\mathbf{h}_2$ geometry where dissociative adsorption over an energy barrier of 0.16 eV is possible. Again, this can be understood by the fact that the hydrogen molecule dissociates towards the direction pointing to the Pd atoms and close to the S atoms. Thus the direct interaction between the H and S atoms leads to the disappearance of the shallow minimum along this path ($E_{ad}=0.20 \text{ eV}$) at the clean Pd(100) surface.

3. 2-D cuts through the PES at top sites above Pd or S atoms

The PES for dissociative adsorption over the $\mathbf{t}_{\text{Pd}}, \mathbf{t}_{\text{S}}$ sites near the adsorbed sulfur is significantly different from the PES at the $\mathbf{h}_1, \mathbf{h}_2,$ and \mathbf{b}_1 sites that are further away from the adsorbed sulfur. Figure 5(a) shows the PES for the $\mathbf{h}_2\text{-}\mathbf{t}_{\text{Pd}}\text{-}\mathbf{h}_2$ geometry. At the clean surface, this dissociation pathway has a local minimum of -0.24 eV in the entrance channel and an energy barrier of 0.15 eV in the exit channel [see Fig. 2(c) of Ref. 8]. The adsorbed sulfur atom is about 2 \AA away from the adsorption site \mathbf{t}_{Pd} and 1.24 \AA above the topmost Pd layer. One can expect that the hydrogen molecule will interact directly the S atom before it reaches the topmost Pd layer; this therefore raises the energy of the PES.

Indeed one can see from Fig. 5(a) that, upon the adsorption of the S adlayer, the local minimum of PES in the entrance channel has disappeared and the energy barrier in the exit channel has raised to 1.28 eV even though the dissociation of hydrogen atoms does not point towards the adsorbed sulfur atoms.

Figure 5(b) shows the PES at the \mathbf{t}_{S} site within $\mathbf{b}_2\text{-}\mathbf{t}_{\text{S}}\text{-}\mathbf{b}_2$ geometry. In this geometry, the hydrogen molecule

directly approaches the S atom on the surface which results in a strong repulsion. Seen from Fig. 5(b), we found that the PES has increased to more than 1.5 eV even when the molecule is still 3 \AA above the topmost Pd layer. However, we found an energy minimum of 1.58 eV at $(Z, d_{\text{H-H}})=(2.20 \text{ \AA}, 1.90 \text{ \AA})$. Judging from the fact that the hydrogen atoms are 2.20 \AA above the topmost Pd layer, we believe that this energy minimum is completely caused by the local bonding properties between the H and S atoms.

From the facts found in Figure 5, one can expect that if the projected distance d_{\parallel} (parallel to surface) between the adsorption site and the adsorbed sulfur atom is smaller than 2 \AA , the dissociation behavior of the hydrogen molecule is dominated by the strong repulsive interaction between H and S atoms. This can be further proved by studying the PES of a frozen H_2 molecule (i.e., $d_{\text{H-H}}=\text{const}$) above the sulfur covered surface. Figure 6 shows the PES of a hydrogen molecule with $d_{\text{H-H}}=0.76 \text{ \AA}$ with its center of mass moving inside the (010) plane crossing the $\mathbf{h}_1, \mathbf{t}_{\text{Pd}}, \mathbf{t}_{\text{S}}$ adsorption sites. This PES is defined as $(X, Y, Z, d, \theta, \phi)=(t/\sqrt{2}, t/\sqrt{2}, Z, 0.76 \text{ \AA}, 90^\circ, 135^\circ)$, where t is the projected distance of the hydrogen center of mass from the sulfur atom in the (100) plane given in \AA .

As one can see from Figure 6, the potential energy of the hydrogen molecule increases significantly when the molecule comes close to the sulfur or the palladium atoms. The semi-circles in Figure 6 indicate the positions where the center-of-mass of the molecule is 1.5 \AA away from the S atom or 1.2 \AA away from the Pd atom, respectively. The potential energy of the hydrogen molecule at this distance has increased to values larger than 1.5 eV. This shows the strong inhibition of the hydrogen dissociation in the vicinity of the sulfur and palladium atoms.

Summarizing the results for the H_2 dissociation on the (2×2) S covered Pd(100) surface, over the $\mathbf{h}_1, \mathbf{h}_2, \mathbf{b}_1, \mathbf{t}_{\text{Pd}}, \mathbf{t}_{\text{S}}$ sites we found that the dissociation behavior of H_2 molecule strongly depends on the projected distance d_{\parallel} between the hydrogen center of mass and the adsorbed sulfur atom, and on the orientation of the dissociating molecule. The dissociation behavior of hydrogen over the the (2×2) S covered Pd(100) surface can be summarized as follows:

(1) For the geometry where the molecule reaches the surface at a position more than 3 \AA away from the sulfur atom, i.e. $d_{\parallel} \geq 3 \text{ \AA}$ (e.g. at the \mathbf{h}_1 site), the dissociation is activated and the energy barrier is about 0.1 eV in the entrance channel resulting from the sulfur-induced modification of the local electronic structure at the surface (see the elbow plots of $\mathbf{b}_1\text{-}\mathbf{h}_1\text{-}\mathbf{b}_1$ and $\mathbf{t}_{\text{Pd}}\text{-}\mathbf{h}_1\text{-}\mathbf{t}_{\text{Pd}}$ geometry).

(2) For the geometry where the molecule reaches the surface at a position about $\sim 2.7 - 3.2 \text{ \AA}$ away from the S atom (e.g. at the \mathbf{h}_2 or \mathbf{b}_1 sites), if the molecule is oriented so that the hydrogen atoms do not approach the adsorbed sulfur, the dissociation is also activated. The energy barrier is in the entrance channel and its

magnitude depends on the distance of the molecule from the S atoms. For the $\mathbf{h}_1\text{-b}_1\text{-h}_2$ geometry, the energy barrier is 0.16 eV, whereas the barrier height is 0.6 eV for the $\mathbf{b}_2\text{-h}_2\text{-b}_2$ geometry because the latter adsorption position is closer to the sulfur atom.

(3) For the geometry where the molecule reaches the surface at a position about $\sim 2.7 - 3.2 \text{ \AA}$ away from the sulfur atom (e.g. at the \mathbf{h}_2 or \mathbf{b}_1 sites), if the molecule is oriented so that the hydrogen atoms approach sulfur atoms, the dissociation becomes purely repulsive due to the direct interaction between H_2 and the S atoms (see the PES plots of $\mathbf{b}_2\text{-h}_2\text{-b}_2$ and $\mathbf{t}_{\text{Pd}}\text{-b}_1\text{-t}_{\text{Pd}}$ geometry).

(4) For the geometry where the projected distance d_{\parallel} is about $\sim 1.8 - 2.3 \text{ \AA}$ and if the molecule is oriented so that the hydrogen atoms do not approach the adsorbed sulfur, the dissociation behavior of the hydrogen molecule is activated, however, with high energy barriers ($\geq 1.2 \text{ eV}$) created by the strong repulsive interaction between hydrogen and sulfur (see the PES of $\mathbf{h}_2\text{-t}_{\text{Pd}}\text{-h}_2$ geometry).

(5) For the geometry where the projected distance d_{\parallel} is smaller than 1.5 \AA , the dissociation behavior of the hydrogen molecule will be dominated by the strong repulsive interaction between H and S atoms and becomes activated with a high energy barrier ($\geq 2.5 \text{ eV}$) (see PES of $\mathbf{b}_2\text{-t}_S\text{-b}_2$) or purely repulsive if one of the H atoms points to the S atom.

(6) For the geometry where the molecule is in an upright geometry with its molecular axis perpendicular to the surface, the PES is repulsive.

In Table II we summarize the results of the adsorption energies and dissociation barriers at six different geometries at the (2×2) sulfur covered surface and at the clean surface. For the clean Pd(100) surface, most of the hydrogen dissociation pathways are non-activated if the H_2 molecule dissociates parallel to the surface ($\theta=90^\circ$), and only a few dissociation pathways are activated for this molecular orientation with small energy barriers ($\leq 0.15 \text{ eV}$). It was explained by Gross, Wilke, and Scheffler²⁶ that the large initial sticking coefficient (~ 0.7) of low energy hydrogen molecules on the Pd(100) surface¹² is mainly due to the steering effect. For the (2×2) sulfur covered surface, it is interesting to see that all the dissociation pathways become activated with energy barriers ranging from 0.1 eV to 2.55 eV. This fact explains qualitatively the reason why the sticking coefficient of H_2 is strongly reduced upon the adsorption of sulfur adatoms, however, a detailed understanding needs a 6-D quantum dynamical calculation²⁶ and will be published later.³²

In order to understand the different origin of the formation of small energy barriers at the \mathbf{h}_1 and \mathbf{b}_1 sites and large energy barriers at \mathbf{t}_{Pd} , \mathbf{t}_S sites, we compare the density of states (DOS) for the H_2 molecule in different geometries. Figure 7(a) shows the DOS when the H_2 molecule is in the $\mathbf{t}_{\text{Pd}}\text{-h}_1\text{-t}_{\text{Pd}}$ configuration. The H-H distance is taken as 0.75 \AA and the center of mass of the H_2 molecule is 4.03 \AA above the topmost Pd layer such that there is no interaction between the hydrogen

molecule and the sulfur covered palladium surface. It is evident that the sulfur p orbitals strongly interact with the Pd d states, giving rise to a narrow peak just below the Pd d band edge (at $\epsilon-\epsilon_F = -4.8 \text{ eV}$) and a broad band at higher energies which has substantial DOS at the Fermi level. The d band at the surface Pd atoms is broadened due to the interaction with the S atoms.

In Fig. 7(a), one intense peak of the DOS at the H atoms is found at the energy of the sulfur related bonding state at -4.8 eV . This degeneracy is accidental, however. There exists no broad distribution of states just below the Fermi level. This indicates that at this height above the surface, the σ_g orbital of the H_2 molecule interacts neither with the sulfur related bonding state nor with the surface Pd d band.

When the H_2 molecule gradually approaches the surface, the interaction of the hydrogen states with the sulfur related bonding state and the surface Pd d states begins to build up. The intense peak of the DOS at -4.8 eV diminishes quickly and splits into a sharp bonding state and anti-bonding broad band just below the Fermi level. In Fig. 7(b) where the H_2 molecule is 1.61 \AA above the topmost Pd layer, the intense DOS of the H atoms found at -4.8 eV has shifted. The interaction of the σ_g orbital of the H_2 molecule with the broad band of the surface Pd d states results in a sharp bonding state of the H_2 σ_g -surface interaction at -7.1 eV and a broader distribution of states with substantial weight below the Fermi level. Consequently we encounter an occupation of the H_2 -substrate antibonding states. Thus, a repulsive contribution to the H_2 -surface interaction appears and gives rise to the formation of a small energy barrier.

Figure 7(c) shows the DOS of the H_2 molecule in the $\mathbf{b}_2\text{-t}_S\text{-b}_2$ geometry. The H-H distance is taken as 0.75 \AA and the center of mass of the H_2 molecule is 3.38 \AA above the topmost Pd layer. It is interesting to see that at this height a strong interaction is already found between the hydrogen molecule and the adsorbed sulfur. The intense peak of DOS at -4.8 eV has split into a sharp bonding state at (-6.6 eV) and a narrow anti-bonding state (at -4.0 eV) that strongly indicates the direct interaction of the H_2 σ_g orbital with the sulfur related $2 p$ state at -4.8 eV which leads to a large energy barrier.

Summarizing the above results and analysis, we conclude that the non-activated dissociation at clean Pd(100) surface is inhibited upon the adsorption of a (2×2) sulfur adlayer. The dissociative adsorption of hydrogen with its molecular axis parallel to the surface is strongly corrugated; it has a wide range of energy barriers ($0.10 - 0.15 \text{ eV}$ near the \mathbf{h}_1 and \mathbf{b}_2 sites; 0.6 eV near the \mathbf{h}_2 site; 1.4 eV near the \mathbf{t}_{Pd} site; 2.6 eV near \mathbf{t}_S) that strongly depends on the projected distance d_{\parallel} between H_2 and the S atoms, it also depends on the molecular orientation ϕ . Still dissociative adsorption of hydrogen is an exothermic process. Thus the poisoning effect of sulfur adatoms for H_2 dissociation at low sulfur coverage ($\Theta_S \leq 0.25$) is governed by the formation of energy barriers and not by the blocking of adsorption sites. To our knowl-

edge, this is the most corrugated surface for dissociative adsorption studied so far by *ab initio* calculations. This has interesting consequences for the dissociation dynamics on this PES.³²

IV. H₂ AT THE c(2×2) SULFUR COVERED Pd(100) SURFACE

A. Determination of the potential energy surface (PES)

The potential energy surface for the dissociative adsorption of hydrogen over the sulfur covered c(2×2) Pd(100) surface is described within the same set of coordinates ($X, Y, Z, d_{\text{H-H}}, \theta, \phi$) as used for the (2×2) surface (see Figure 8). Figure 9 shows the surface unit cell for the c(2×2) sulfur covered Pd(100) surface. Inside the unit cell, we specifically analyse the dissociation at the following sites: bridge site (denoted by **b**), hollow site (denoted by **h**), top site above the Pd atom (denoted by **t_{Pd}**), and top site above the S atom (denoted by **t_S**). To obtain a detailed information about the interaction, we have again calculated the elbow-plots at different sites and different molecular orientations (θ, ϕ).

B. Results

For the c(2×2) S covered surface, the adsorbed S atoms form a 4 Å × 4 Å square lattice 1.29 Å above the Pd layer.³¹ From that it follows that the projected distance d_{\parallel} of the molecule from one sulfur adatom cannot be larger than 2.85 Å. Thus the hydrogen molecules on the Pd surface have to dissociate close to the sulfur atoms no matter how they approach the surface. Therefore, from what we have learned in the last section about the dissociation behavior of H₂ over the (2×2) S covered surface, we might expect for the c(2×2) S covered surface that the dissociation will become purely repulsive for all different sites and orientations. Indeed, this is what we find from our *ab initio* calculations.

1. 2-D cuts through the PES at the hollow site

At the **h** site, the projected distance d_{\parallel} between this site and the sulfur atom is 2.85 Å. However, there are four S atoms near this site so that a dissociating hydrogen molecule will always approach sulfur atoms. One can thus expect that the dissociation is purely repulsive for the hollow site. Figures 10(a), 10(b), and 10(c) show the PES for the **t_{Pd}-h-t_{Pd}**, the **b-h-b**, and the (X, Y, θ, ϕ) = (0.5a, 0.5a, 0°, 0°) geometries at the hollow site, respectively. Figure 10 shows that the potential energy has increased to about 1.5 eV when the hydrogen molecule is at the same height above the Pd surface as the S atoms

($Z=1.29$ Å). As mentioned above, this increase is due to the strong repulsive interaction between H and S atoms.

2. 2-D cuts through the PES at top sites over Pd and S atoms

At the **t_{Pd}** site, the projected distance d_{\parallel} to the nearest sulfur atom is only 2.0 Å. Again we can expect that the strong repulsion between the H₂ and the S atoms will dominate the dissociation behavior of the molecule. Figures 11(a) and 11(b) show the PES for the **h-t_{Pd}-h** and **t_S-t_{Pd}-t_S** geometries at the **t_{Pd}** site. We find that the potential energy has increased to more than 2.0 eV even when the hydrogen molecule is at a height of $Z=1.8$ Å above the Pd atoms which is still 0.5 Å above the sulfur adlayer.

Figure 11(c) shows the PES at the **t_S** site within the **b-t_S-b** geometry. In this geometry, the hydrogen molecule approaches the surface directly towards the S atom. The potential energy increases dramatically to more than 1.5 eV when the molecule is still 3 Å above the topmost Pd layer. At this geometry the PES of the c(2×2) surface is found to be very similar to the PES of the (2×2) surface at the **b₂-t_S-b₂** geometry. We find an energy minimum of 1.56 eV (at $Z=2.20$ Å, $d_{\text{H-H}}=1.90$ Å) as for the (2×2) surface. The fact that the PES of the (2×2) and the c(2×2) for this particular configuration are very similar shows that the hydrogen interaction with a sulfur covered surface close to the sulfur atoms is completely determined by the local bonding properties between the H and S atoms.

Summarizing the results for the **h**, **t_{Pd}**, and **t_S** sites, we find that the dissociation behavior of H₂ at the c(2×2) S covered Pd(100) surface is dominated by the strong direct interaction between hydrogen and sulfur atoms. The PES for hydrogen dissociation is repulsive and endothermic due to the fact that for all different approach geometries the hydrogen molecules come close to the sulfur adatoms before the dissociation is completed.

V. DEPENDENCE OF THE PES ON THE POLAR ANGLE θ AND THE AZIMUTHAL ANGLE ϕ OF THE HYDROGEN MOLECULE

The two-dimensional cuts through the PES described in the section III and IV refer to the situation where the orientation of molecular axis is parallel or perpendicular to the surface. In reality, the molecules impinges on the surface with all possible orientations. At the clean Pd(100) surface, Wilke and Scheffler⁸ have shown that at the **h-b-h** adsorption geometry the change of the orientation of the molecular axis with respect to the surface normal θ away from $\theta = 90^\circ$ implies a significant increase in the potential energy. This increase was found to be proportional to $\cos^2 \theta$. Eichler, Kresse, and Hafner⁹ have

found for the Rh(100) surface at less symmetric positions (halfway between bridge- and on-top position) that the potential energy also varies similar to the $\cos^2\theta$ behavior but with the minimum of the energy shifted by $15^\circ \sim 20^\circ$ from the parallel orientation of the molecule.

To analyze the energy variation with θ for the (2×2) sulfur covered Pd(100) surface, we first chose one high symmetry point $(Z, d_{\text{H-H}}) = (1.05 \text{ \AA}, 1.0 \text{ \AA})$ within the $\mathbf{b}_1\text{-h}_1\text{-b}_1$ geometry and calculated the potential energy dependence on the angle θ at this site. Figure 12 shows the energy variation with θ which is well described by $\cos^2\theta$. To further analyze the energy variation with θ at less symmetric points, we chose the two points $(Z, d_{\text{H-H}}) = (1.52\text{ \AA}, 0.8\text{ \AA})$, and $(Z, d_{\text{H-H}}) = (1.05\text{ \AA}, 1.0\text{ \AA})$ at the $\mathbf{h}_1\text{-b}_1\text{-h}_2$ geometry and calculated their energy dependence on θ . The results are shown in Fig. 13. The potential energy is plotted as a function of $\cos^2(\theta - \theta_0)$ for values of θ between $0^\circ \leq \theta \leq 180^\circ$. Due to the lower symmetry, the potential energy is no longer single-valued in this representation as in the high-symmetry situation of Fig. 12 with $\theta_0 = 0$, but it is double-valued. The fact that the corresponding results fall upon one line indicates that the energy variation is well described by $\cos^2(\theta - \theta_0)$ with $\theta_0 \approx 2^\circ - 5^\circ$. These findings are similar to the ones found for Rh(100) by Eichler and coworkers.⁹

The Figs. 12 and 13 demonstrate the significant increase in the potential energy by rotating the molecule away from $\theta = 90^\circ$, which is true at any point of the surface. This has been already indicated by the comparison of the PES of the hydrogen molecule approaching the hollow \mathbf{h}_1 site in the $\mathbf{t}_{\text{Pd}}\text{-h}_1\text{-t}_{\text{Pd}}$ geometry [see Fig. 3(b)] with the PES of the hydrogen molecule at the same \mathbf{h}_1 site in an upright position [see Fig. 3(d)]. It is evident that rotating the molecule axis perpendicular to the surface increases the energy at the entrance channel and changes the dissociation pathway from being activated [see Fig. 3(b)] to being purely repulsive.

The effect of the azimuthal angle ϕ on the hydrogen dissociation can be seen by comparing the PES for the $\mathbf{t}_{\text{Pd}}\text{-h}_1\text{-t}_{\text{Pd}}$ adsorption geometry [see Fig. 3(b)] with the $\mathbf{b}_1\text{-h}_1\text{-b}_1$ adsorption geometry [see Fig. 3(a)]. For these two geometries at the \mathbf{h}_1 site, the projected distance of the H_2 center of mass from any sulfur atom is about 4 \AA and the two elbow plots are very similar at the entrance channel because the hydrogen atoms are still far away from any Pd or S atoms. However, differences are found at the exit channel because the hydrogen atoms dissociate towards the Pd atoms in the $\mathbf{t}_{\text{Pd}}\text{-h}_1\text{-t}_{\text{Pd}}$ geometry whereas they dissociate towards the bridge site for the $\mathbf{b}_1\text{-h}_1\text{-b}_1$ geometry.

The dependence of the PES on the azimuthal angle is even more dramatic at adsorption sites close to the adsorbed sulfur. For example, if we compare the PES at the \mathbf{h}_2 site in the $\mathbf{b}_2\text{-h}_2\text{-b}_2$ geometry [see Fig. 3(c)] with the $\mathbf{b}_1\text{-h}_2\text{-b}_1$ geometry [see Fig. 1(c) of Ref. 10], we can see that rotating the molecule towards the sulfur atoms leads to a large increase in the potential energy and changes the dissociation from being activated to being

purely repulsive. In conclusion, we expect a significant increase of the potential energy by rotating the molecule towards sulfur atoms if the projected distance d_{\parallel} of the H_2 center of mass from the sulfur atoms is smaller than 2.85\AA.

VI. ANALYTICAL REPRESENTATION OF THE *ab initio* PES FOR H_2 AT $\text{S}(2\times 2)/\text{Pd}(100)$

In order to perform dynamical calculation on the *ab initio* PES, one needs a continuous analytical representation of the PES.²⁷ Details of such an representation for the PES of H_2 on the clean Pd(100) surface have already been published.²⁷ For the H_2 dissociation on the (2×2) sulfur covered Pd(100) surface we have now also determined an analytical representation which has been based upon the analytical PES for the clean surface. However, due to the larger unit cell of the $\text{S}(2\times 2)/\text{Pd}(100)$ surface, the analytical form has been expanded up to the fourth-order Fourier coefficient in the lateral directions parallel to the surface. In addition, in the azimuthal dependence of the PES the fourth-order term (proportional to $\cos(4\phi)$) has also been included.

For the solution of the time-independent Schrödinger equation it is necessary to transform the coordinates in the Zd -plane into reaction path coordinates s and ρ .²⁷ In these coordinates the function $V(X, Y, s, \rho, \theta, \phi)$, which describes the potential energy surface, has the following form in our parametrization:

$$V(X, Y, s, \rho, \theta, \phi) = V^{\text{corr}} + V^{\text{rot}} + V^{\text{vib}} \quad (1)$$

with

$$V^{\text{corr}} = \sum_{m,n=0}^4 V_{m,n}^{(1)}(s) \cos mGX \cos nGY, \quad (2)$$

$$\begin{aligned} V^{\text{rot}} = & \sum_{m=0}^2 V_m^{(2)}(s) \frac{1}{2} \cos^2 \theta (\cos mGX + \cos mGY) \\ & + \sum_{n=1}^2 V_n^{(3)}(s) \frac{1}{2} \sin^2 \theta \cos 2\phi (\cos nGX - \cos nGY) \\ & + V^{(4)}(s) \frac{1}{2} \sin^4 \theta \cos 4\phi (\cos GX + \cos GY) \end{aligned} \quad (3)$$

and

$$V^{\text{vib}} = \frac{\mu}{2} \omega^2(s) [\rho - \Delta\rho(X, Y, s)]^2. \quad (4)$$

$G = 2\pi/a$ is the length of the basis vectors of the square surface reciprocal lattice, a is the nearest neighbor distance between S atoms in the $(2\times 2)\text{S}/\text{Pd}(100)$ surface unit cell and $\omega(s)$ is the vibrational frequency. In addition, the curvature $\kappa = \kappa(s)$ of the minimum energy path has to be determined. The displacement $\Delta\rho$ in the potential

term V^{vib} (Eq. 4) takes into account that the location of the minimum energy path in the Zd -plane depends on the cut through the six-dimensional configuration space. $\Delta\rho$ does not influence the barrier distribution, however, it changes the curvature of the minimum energy paths in the Zd -planes. Large values of $\Delta\rho$ make the quantum dynamical calculations rather time-consuming since they require a large number of vibrational eigenfunctions in the expansion of the hydrogen wave function.²⁷ However, the large values of $\Delta\rho$ only occur for large separations of the hydrogen atoms where they do not influence the calculated sticking probabilities and scattering properties significantly.²⁷ Therefore we have parametrized the displacement properly only for values of $|\Delta\rho| \leq 0.15$ Å.

For the two hydrogen atoms in adjacent adsorption positions, the energetic cost to turn the molecule upright has not been determined by the *ab initio* calculations. This energy enters the term $V_0^{(2)}$ in V_{rot} (Eq. 3). Still it is possible to estimate that energy cost. In the harmonic approximation we can write the potential for the vibrations of the two hydrogen atoms perpendicular to the surface as

$$V_{\text{perp}}(z_1, z_2) = \frac{m}{2}\omega_{\text{ad}}^2(z_1^2 + z_2^2), \quad (5)$$

where z_1 and z_2 denote the z -coordinates of the two hydrogen atoms, m is the mass of the hydrogen atom, and ω_{ad} is the vibrational frequency. Now we transform V_{perp} to the center-of-mass coordinate $Z = (z_1 + z_2)/2$ and the relative coordinate $z = z_2 - z_1$. Then V_{perp} becomes

$$V_{\text{perp}}(Z, z) = \frac{M}{2}\omega_{\text{ad}}^2 Z^2 + \frac{\mu}{2}\omega_{\text{ad}}^2 z^2 \quad (6)$$

with the total mass $M = 2m$ and the reduced mass $\mu = m/2$. The frequency ω_{ad} can be determined from the two-dimensional cuts of the *ab initio* calculations. Comparing V_{rot} and V_{perp} and using $z = \cos\theta d_{H-H}$, we obtain for $V_0^{(2)}$ at adjacent atomic adsorption positions

$$V_0^{(2)}(s = s_{\text{ad}}) = \frac{\mu}{2}\omega_{\text{ad}}^2 d_{H(\text{ad})-H(\text{ad})}^2 \quad (7)$$

$V_0^{(2)}$ is therefore parametrized in such a way that it approaches the value of Eq. 7 for the dissociated molecule on the surface.

In general the functions $V_{m,n}^{(i)}(s)$ and $\omega(s)$ are determined such that the difference to the *ab initio* calculations on the average is smaller than 50 meV. The energies are particularly well described along the minimum energy paths of the two-dimensional cuts of the six-dimensional configuration space. The maximum error of the analytical representation in comparison to the *ab initio* PES is of the order of 0.5 eV. This error, however, does only occur for large distances from the minimum energy path where the potential energy is already rather high. Therefore the maximum error has only very little influence on the dynamical calculations. In Fig. 14 we have plotted

two cuts through the analytical six-dimensional PES for the $\mathbf{b}_1\text{-h}_1\text{-b}_1$ and the $\mathbf{h}_2\text{-t}_{\text{Pd}}\text{-h}_2$ geometries, respectively. They should be compared with the corresponding *ab initio* cuts in Fig. 3 and Fig. 5.

VII. CONCLUSION

We have performed detailed calculations of the PES for the dissociative adsorption of hydrogen molecules on the (2×2) and the $c(2\times 2)$ sulfur covered Pd(100) surface using density-functional theory and the full-potential linear-augmented plane wave method.^{29,30} The exchange correlation is treated in the generalized gradient approximation (GGA).²⁸ For the H_2 dissociation on the (2×2) S covered Pd(100) surface, by calculating the PES over different adsorption sites we find that the non-activated dissociation pathways at the clean Pd(100) surface become activated or purely repulsive upon the adsorption of a (2×2) sulfur adlayer. The PES is strongly corrugated. The minimum barrier has a height of 0.1 eV, while close to the S atoms the barrier towards dissociative adsorption for molecules with their axis parallel to the surface becomes larger than 2.5 eV. We find that the energy variation with the polar angle θ of the hydrogen molecule at the \mathbf{h}_1 and \mathbf{b}_1 sites is well described by $\cos^2(\theta - \theta_0)$ with $\theta_0 \approx 0^\circ - 5^\circ$. We also find that the PES strongly depends on the molecular azimuthal orientation ϕ if the projected distance of H_2 from the adsorbed sulfur is smaller than 2.85 Å. Still the dissociative adsorption of hydrogen is exothermic; thus the poisoning effect of sulfur adatoms for H_2 dissociation at low sulfur coverage ($\Theta_{\text{S}} \leq 0.25$) is governed by the formation of energy barriers, not by blocking of the adsorption sites.

For the $c(2\times 2)$ S covered Pd(100) surface, the results of our calculations indicate that the interaction of H_2 with this surface is dominated by the strong repulsion between H_2 and the sulfur atoms. On the $c(2\times 2)$ S covered Pd(100) surface the sulfur atoms form a $4 \text{ \AA} \times 4 \text{ \AA}$ square lattice above the topmost Pd layer; therefore, all molecules that reach the surface will eventually approach some adsorbed sulfur atoms before the dissociation is complete. Due to this fact, non-activated reaction pathways at the clean Pd(100) surface are completely inhibited, and all dissociation pathways are purely repulsive.

ACKNOWLEDGMENTS

C. M. Wei would like to acknowledge the one-year financial support from the National Science Council of the Republic of China.

- * Permanent address: Institute of Physics, Academia Sinica, Nankang, Taipei, Taiwan 11529, Republic of China.
- ¹ B.I. Lundqvist, O. Gunnarsson, H. Hjelmberg, and J.K. Nørskov, *Surf. Sci.* **89**, 196 (1979).
 - ² J.K. Nørskov, A. Houmoller, P.K. Johansson, and B.I. Lundqvist, *Phys. Rev. Lett.* **46**, 257 (1981).
 - ³ P.J. Feibelman, *Phys. Rev. Lett.* **67**, 461 (1991).
 - ⁴ B. Hammer, M. Scheffler, K.W. Jacobsen, and J.K. Nørskov, *Phys. Rev. Lett.* **73**, 1400 (1994).
 - ⁵ J.A. White, D.M. Bird, M.C. Payne, and I. Stich, *Phys. Rev. Lett.* **73**, 1404 (1994).
 - ⁶ B. Hammer and M. Scheffler, *Phys. Rev. Lett.* **74**, 3487 (1995).
 - ⁷ J.A. White, D.M. Bird, and M.C. Payne, *Phys. Rev. B* **53**, 1667 (1996).
 - ⁸ S. Wilke and M. Scheffler, *Phys. Rev. B* **53**, 4926 (1996).
 - ⁹ A. Eichler, G. Kresse, and J. Hafner, *Rev. Lett.* **77**, 1119 (1996).
 - ¹⁰ D.W. Goodman and M. Kiskinova, *Surf. Sci.* **105**, L265 (1981).
 - ¹¹ S. Johnson and R.J. Madix, *Surf. Sci.* **108**, 77 (1981).
 - ¹² K.D. Rendulic, G. Anger, and A. Winkler, *Surf. Sci.* **208**, 404 (1989).
 - ¹³ M.L. Burke and R.J. Madix, *Surf. Sci.* **237**, 1 (1990).
 - ¹⁴ P.J. Feibelman and D.R. Hamann, *Phys. Rev. Lett.* **52**, 61 (1984).
 - ¹⁵ P.J. Feibelman and D.R. Hamann, *Surf. Sci.* **149**, 48 (1985).
 - ¹⁶ J.M. MacLaren, J.B. Pendry, and R.W. Joyner, *Surf. Sci.* **165**, L80 (1986).
 - ¹⁷ B. Hammer and J.K. Nørskov, *Surf. Sci.* **343**, 211 (1995).
 - ¹⁸ S. Wilke, M. Cohen, and M. Scheffler, *Phys. Rev. Lett.* **77**, 1560 (1996).
 - ¹⁹ J.K. Nørskov, S. Holloway, and N.D. Lang, *Surf. Sci.* **137**, 65 (1984).
 - ²⁰ J.K. Nørskov, in *The Chemical Physics of Solid Surfaces*, edited by D.A. King and D.P. Woodruff (Elsevier, Amsterdam, 1993), Vol. 6, p. 1.
 - ²¹ B. Hammer, K.W. Jacobsen, and J.K. Nørskov, *Surf. Sci.* **297**, L68 (1993).
 - ²² S. Wilke and M. Scheffler, *Surf. Sci.* **329**, L605 (1995).
 - ²³ S. Wilke and M. Scheffler, *Phys. Rev. Lett.* **76**, 3380 (1996).
 - ²⁴ G. Comsa, R. David, and B.-J. Schumacher, *Surf. Sci.* **95**, L210 (1980).
 - ²⁵ R.J. Behm, K. Christmann, and G. Ertl, *Surf. Sci.* **99**, 320 (1980).
 - ²⁶ A. Gross, S. Wilke, and M. Scheffler, *Phys. Rev. Lett.* **75**, 2718 (1995).
 - ²⁷ A. Gross and M. Scheffler, *Phys. Rev. B*, in press.
 - ²⁸ J.P. Perdew *et al.*, *Phys. Rev. B* **46**, 6671 (1992).
 - ²⁹ P. Blaha, K. Schwarz, P. Dufek, and R. Augustyn, Technical University of Vienna Report No. WIEN95, 1995.
 - ³⁰ B. Kohler, S. Wilke, M. Scheffler, R. Kouba, and Claudia Ambrosch-Draxl, *Comp. Phys. Commun.* **94**, 31 (1996).
 - ³¹ S. Wilke and M. Scheffler, unpublished.
 - ³² A. Gross, C.M. Wei, and M. Scheffler, to be published.

FIG. 1. Sketch of a coordinate system for the description of the hydrogen molecule above the (2×2) sulfur covered Pd(100) surface. The other coordinates are the height of the center-of-mass of H_2 above the surface Z , the H-H distance d_{H-H} , and the angle of the molecular axis with the surface normal θ .

FIG. 2. Surface geometry of the (2×2) sulfur covered Pd(100) surface with two inequivalent hollow sites h_1 , h_2 , two bridge sites b_1 , b_2 , top site t_{Pd} (above the Pd atom), and t_S (above the S atom).

FIG. 3. Cuts through the six-dimensional potential energy surface (PES) of H_2 dissociation over $(2 \times 2)S/Pd(100)$ at the hollow sites h_1 and h_2 : (a) PES for $b_1-h_1-b_1$ geometry; (b) PES for $t_{Pd}-h_1-t_{Pd}$ geometry; (c) PES for $b_2-h_2-b_2$ geometry; (d) PES for the molecule at the h_1 site with the molecular axis perpendicular to the surface. The energy contours, given in eV per molecule, are displayed as a function of the H-H distance, d_{H-H} , and the height Z of the center-of-mass of H_2 above the topmost Pd layer. All length scales, also in the following, are given in Å. The geometry of each dissociation pathway is indicated above.

FIG. 4. Cuts through the six-dimensional potential energy surface (PES) of H_2 dissociation over $(2 \times 2)S/Pd(100)$ at the bridge site b_1 : (a) PES for $h_1-b_1-h_2$ geometry; (b) PES for $t_{Pd}-b_1-t_{Pd}$ geometry. The geometry of each dissociation pathway is indicated above.

FIG. 5. Cuts through the six-dimensional potential energy surface (PES) of H_2 dissociation over $(2 \times 2)S/Pd(100)$ at the top sites t_{Pd} and t_S : (a) PES for $h_2-t_{Pd}-h_2$ geometry; (b) PES for $b_2-t_S-b_2$ geometry. The geometry of each dissociation pathway is indicated above.

FIG. 6. PES of a hydrogen molecule with $d_{H-H} = 0.76$ Å with its center of mass moving inside the (010) plane crossing the h_1 , t_{Pd} , t_S sites. This PES is defined as $(X, Y, Z, d, \theta, \phi) = (t/\sqrt{2}, t/\sqrt{2}, Z, 0.76\text{Å}, 90^\circ, 135^\circ)$ with t and Z as the two variables given in Å. The variable t is the projected distance of the hydrogen center of mass from the sulfur atom in the (100) plane.

FIG. 7. Density of states (DOS) for a H_2 molecule situated at (a) $(Z, d_{H-H}) = (4.03\text{Å}, 0.75\text{Å})$ within the $t_{Pd}-h_1-t_{Pd}$ geometry; (b) $(Z, d_{H-H}) = (1.61\text{Å}, 0.75\text{Å})$ within the $t_{Pd}-h_1-t_{Pd}$ geometry; (c) $(Z, d_{H-H}) = (3.38\text{Å}, 0.75\text{Å})$ within the $b_2-t_S-b_2$ geometry. Given is the local DOS at the H atoms, the S adatom, the surface Pd atoms, and the bulk Pd atom. The energies are given in eV.

FIG. 8. Sketch of a coordinate system for the description of the hydrogen molecule above the $c(2\times 2)$ sulfur covered Pd(100) surface. The other coordinates are the height of the center-of-mass of H_2 above the surface Z , the H-H distance d_{H-H} , and the angle of the molecular axis with the surface normal θ .

FIG. 9. Surface geometry of the $c(2\times 2)$ sulfur covered Pd(100) surface with hollow site \mathbf{h} , bridge site \mathbf{b} , top site \mathbf{t}_{Pd} above the Pd atom, and top site \mathbf{t}_S above the S atom.

FIG. 10. Cuts through the six-dimensional potential energy surface (PES) of the H_2 dissociation at $c(2\times 2)S/Pd(100)$ at the hollow site \mathbf{h} : (a) PES for $\mathbf{t}_{Pd}-\mathbf{h}-\mathbf{t}_{Pd}$ geometry; (b) PES for $\mathbf{b}_2-\mathbf{h}-\mathbf{b}_2$ geometry; (c) PES for the molecule at the \mathbf{h} site with its axis perpendicular to the surface. The geometry of each dissociation pathway is indicated above.

FIG. 11. Cuts through the six-dimensional potential energy surface (PES) of the H_2 dissociation at $c(2\times 2)S/Pd(100)$ at the top sites \mathbf{t}_{Pd} and \mathbf{t}_S : (a) PES for $\mathbf{h}-\mathbf{t}_{Pd}-\mathbf{h}$ geometry; (b) PES for $\mathbf{t}_S-\mathbf{t}_S-\mathbf{t}_S$ geometry; (c) PES for $\mathbf{b}-\mathbf{t}_S-\mathbf{b}$ geometry. The geometry of each dissociation pathway is indicated above.

FIG. 12. Dependence of the potential energy of the H_2 molecule at the (2×2) sulfur covered Pd(100) surface on the angle θ of its axis with the surface normal. The potential energy is plotted as a function of $\cos^2 \theta$. The configuration for $\theta = 90^\circ$ corresponds to the $\mathbf{b}_1-\mathbf{h}_1-\mathbf{b}_1$ geometry with $(d_{H-H}, Z) = (1.0\text{\AA}, 1.05\text{\AA})$.

FIG. 13. Dependence of the potential energy of the H_2 molecule at the (2×2) sulfur covered Pd(100) surface on the angle θ of its axis with the surface normal shifted by θ_o . The potential energy is plotted as a function of $\cos^2(\theta - \theta_o)$ for values of θ between $0^\circ \leq \theta \leq 180^\circ$, i.e. the potential energy is double-valued in this representation. The configuration for $\theta = 90^\circ$ corresponds to the $\mathbf{h}_1-\mathbf{b}_2-\mathbf{h}_2$ geometry: (a) $(d_{H-H}, Z, \theta_o) = (1.52\text{\AA}, 0.8\text{\AA}, 4.5^\circ)$; (b) $(d_{H-H}, Z, \theta_o) = (1.0\text{\AA}, 1.05\text{\AA}, 2.2^\circ)$.

FIG. 14. Two cuts through the analytical representation of the six-dimensional *ab initio* PES for the $\mathbf{b}_1-\mathbf{h}_1-\mathbf{b}_1$ and the $\mathbf{h}_2-\mathbf{t}_{Pd}-\mathbf{h}_2$ geometries, respectively.

geometry	(Z, d)	3 Pd slab, $E_{\text{cut}}= 11$ Ry	5 Pd slab, $E_{\text{cut}}= 14$ Ry
b₁-h₁-b₁	(0.61 Å, 0.97 Å)	0.28 eV	0.24 eV
h₁-b₁-h₂	(0.08 Å, 2.85 Å)	-0.79 eV	-0.72 eV
	(0.97 Å, 1.14 Å)	0.13 eV	0.08 eV
t_{Pd}-h₁-t_{Pd}	(1.05 Å, 0.94 Å)	-0.02 eV	-0.01 eV
h₂-t_{Pd}-h₂	(1.45 Å, 1.29 Å)	1.30 eV	1.31 eV

TABLE I. Dependence of the potential energy on the thickness of the substrate Pd slab and the cut-off energy at different H₂ geometries. The energies are given per H₂ molecule.

adsorption site and geometry	clean surface ($\Theta_S=0$)	(2×2) surface ($\Theta_S=0.25$)
h₁ (θ, ϕ)=(90°, 90°)	non-activated, $E_{\text{ad}}= 0.46$ eV	activated $E_b= 0.10$ eV
h₂ (θ, ϕ)=(90°, 90°)		activated $E_b= 0.60$ eV
h₂ (θ, ϕ)=(90°, 0°)		repulsive (≥ 0.75 eV)
h₁ (θ, ϕ)=(90°, 135°)	non-activated, $E_{\text{ad}}= 0.23$ eV	activated $E_b= 0.13$ eV
h₁ (θ, ϕ)=(0°, 0°)	no dissociation	repulsive (≥ 0.25 eV)
b₁ (θ, ϕ)=(90°, 90°)	non-activated, $E_{\text{ad}}= 1.22$ eV	activated $E_b= 0.15$ eV
b₂ (θ, ϕ)=(90°, 0°)	no dissociation	repulsive (≥ 0.25 eV)
t_{Pd} (θ, ϕ)=(90°, 135°)	activated, $E_b= 0.16$ eV	activated $E_b= 1.28$ eV
t_S (θ, ϕ)=(90°, 0°)	—	activated $E_b= 2.55$ eV

TABLE II. Summary of the results for adsorption energies and barrier heights for the H₂ dissociation over the clean Pd(100) surface and the (2×2) sulfur covered Pd(100) surface at different adsorption sites and geometries. The energies are given per H₂ molecule.

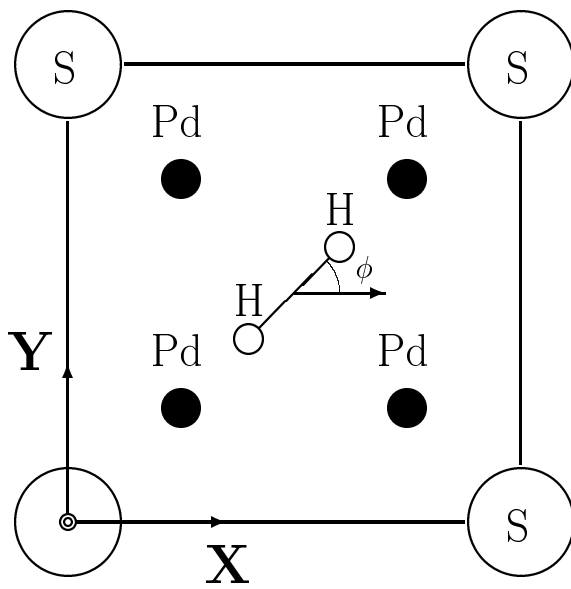


Fig. 1

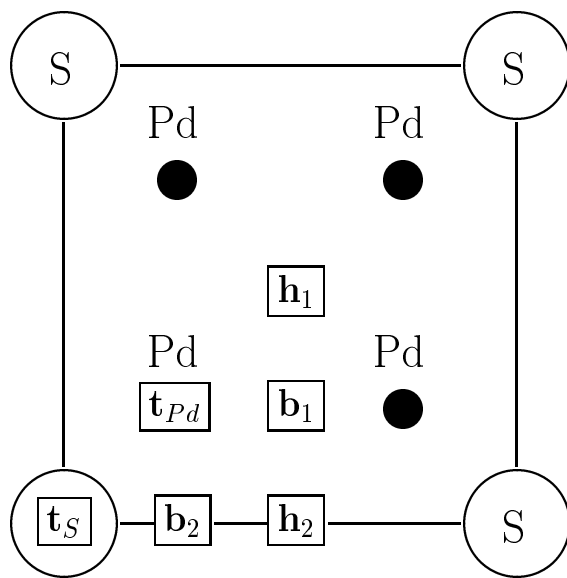


Fig. 2

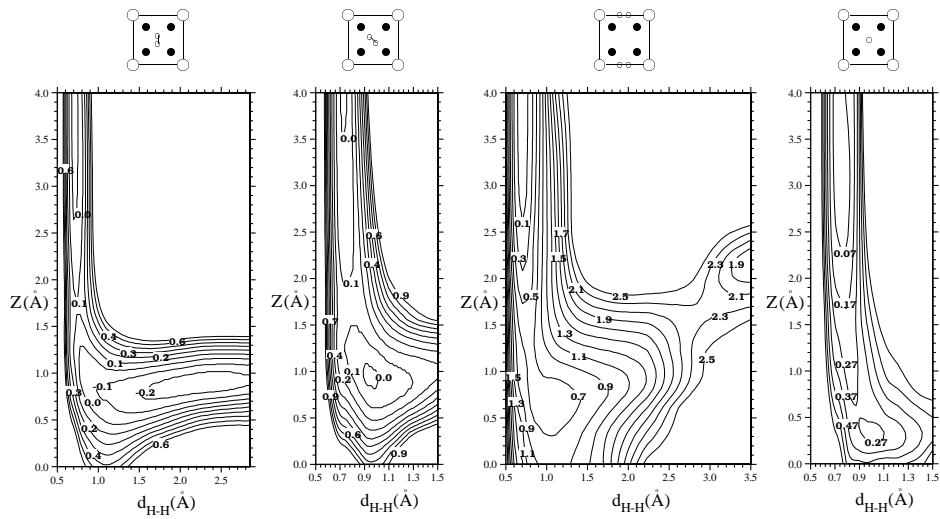


Fig. 3

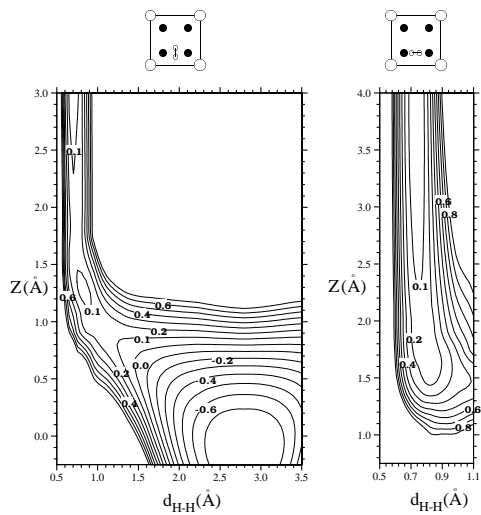


Fig. 4

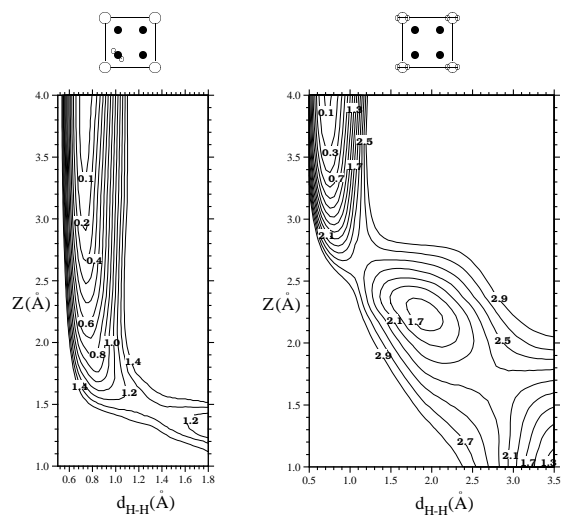


Fig. 5

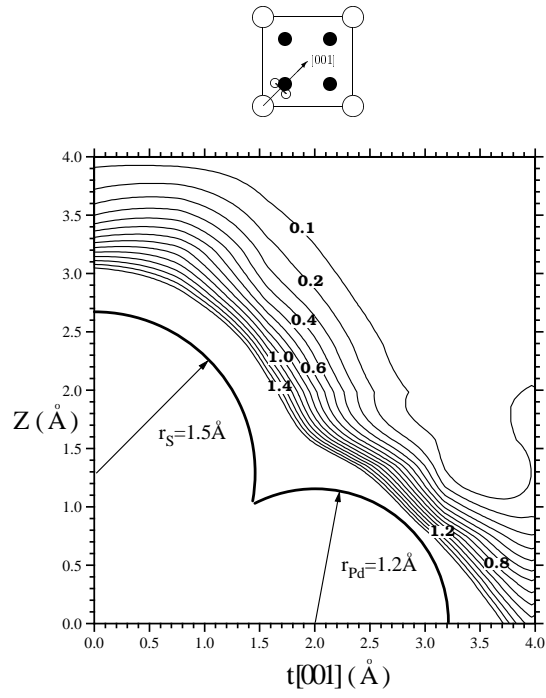


Fig. 6

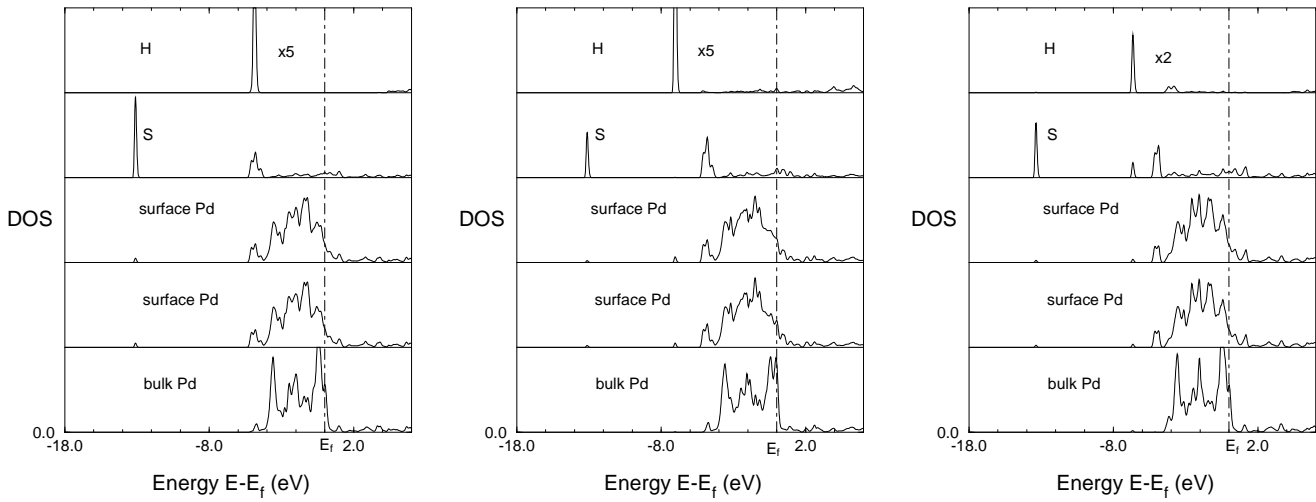


Fig. 7

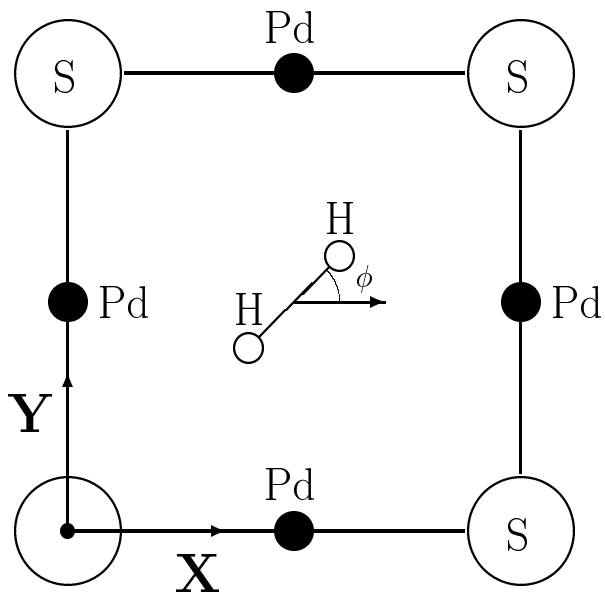


Fig. 8

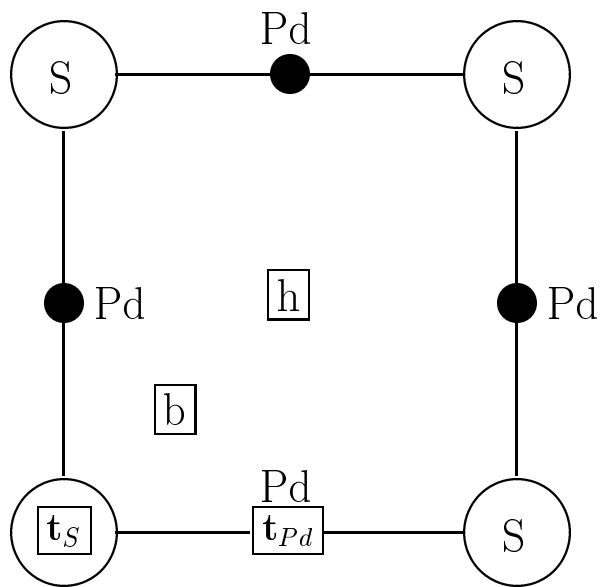


Fig. 9

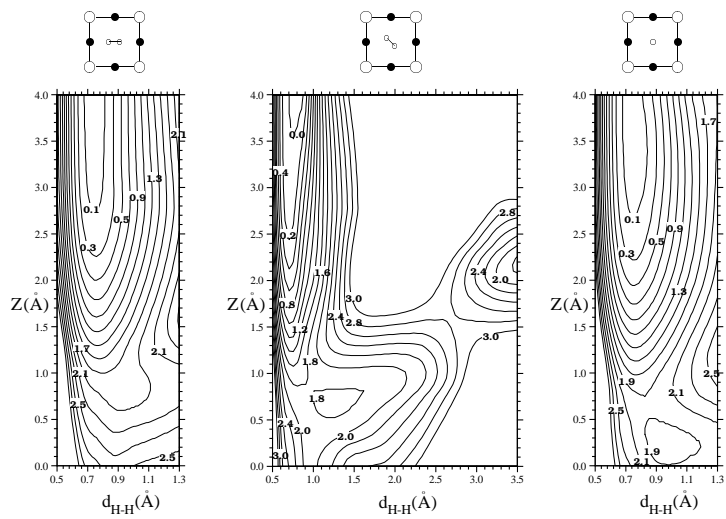


Fig. 10

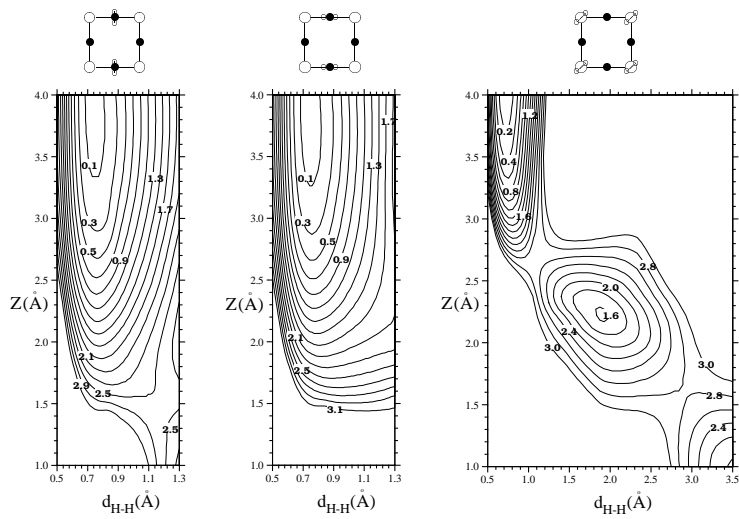


Fig. 11

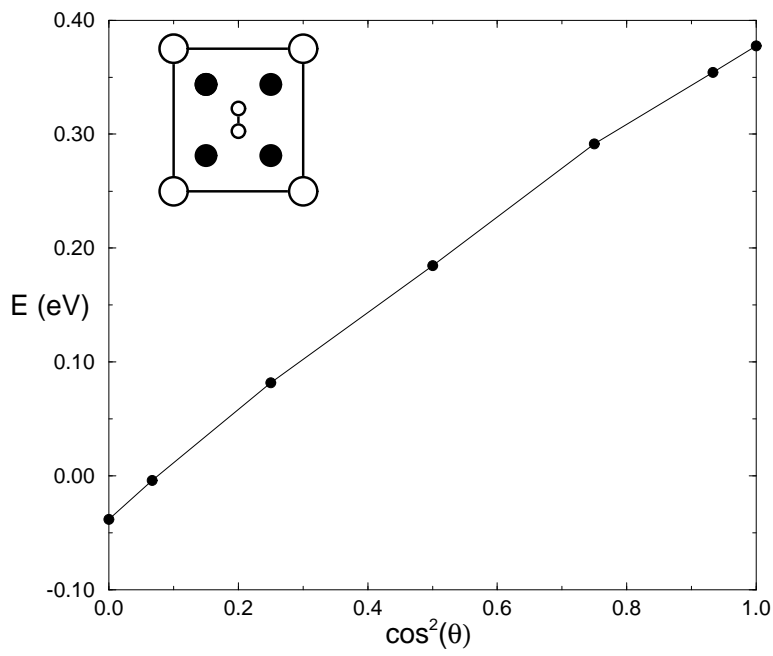


Fig. 12

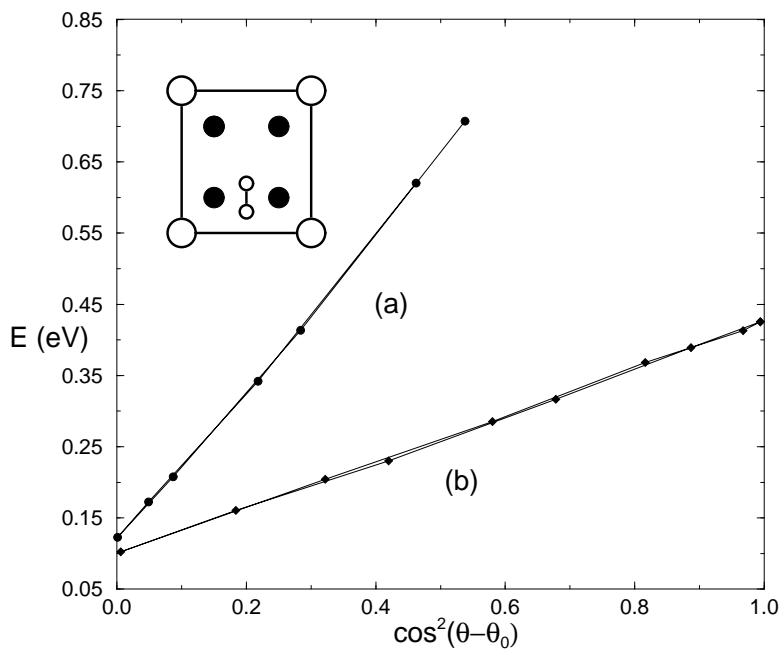


Fig. 13

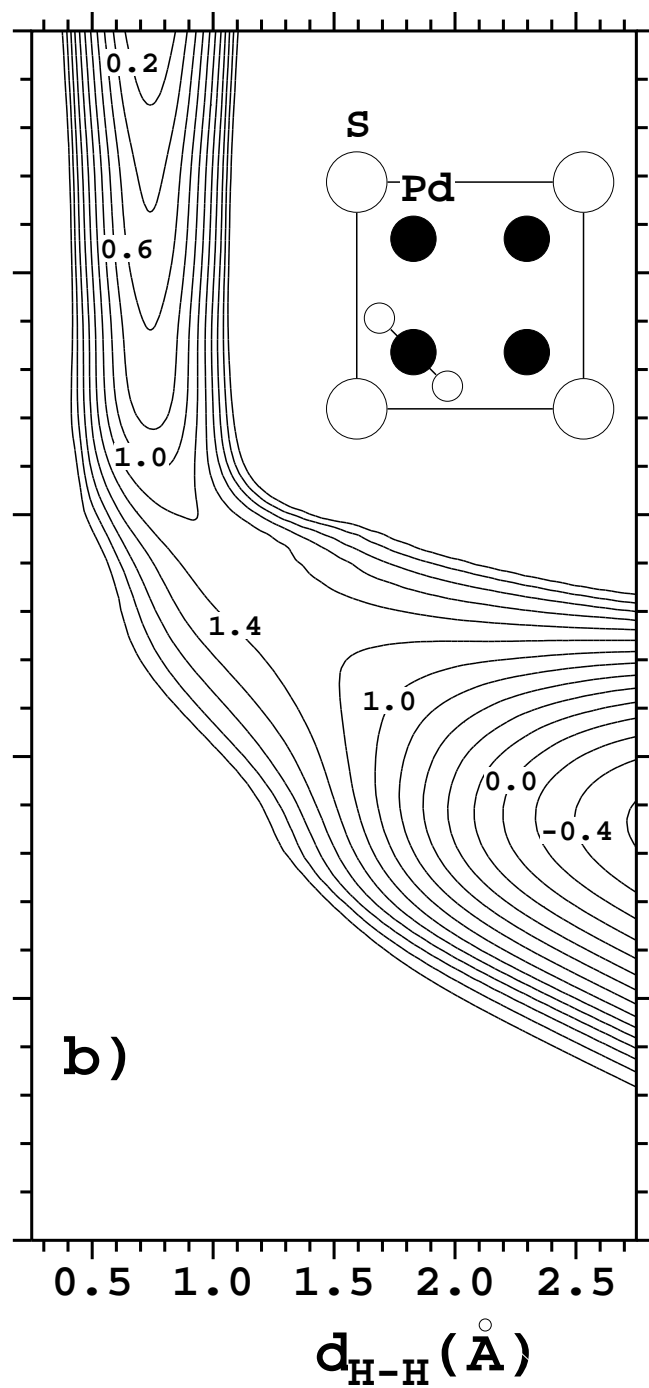
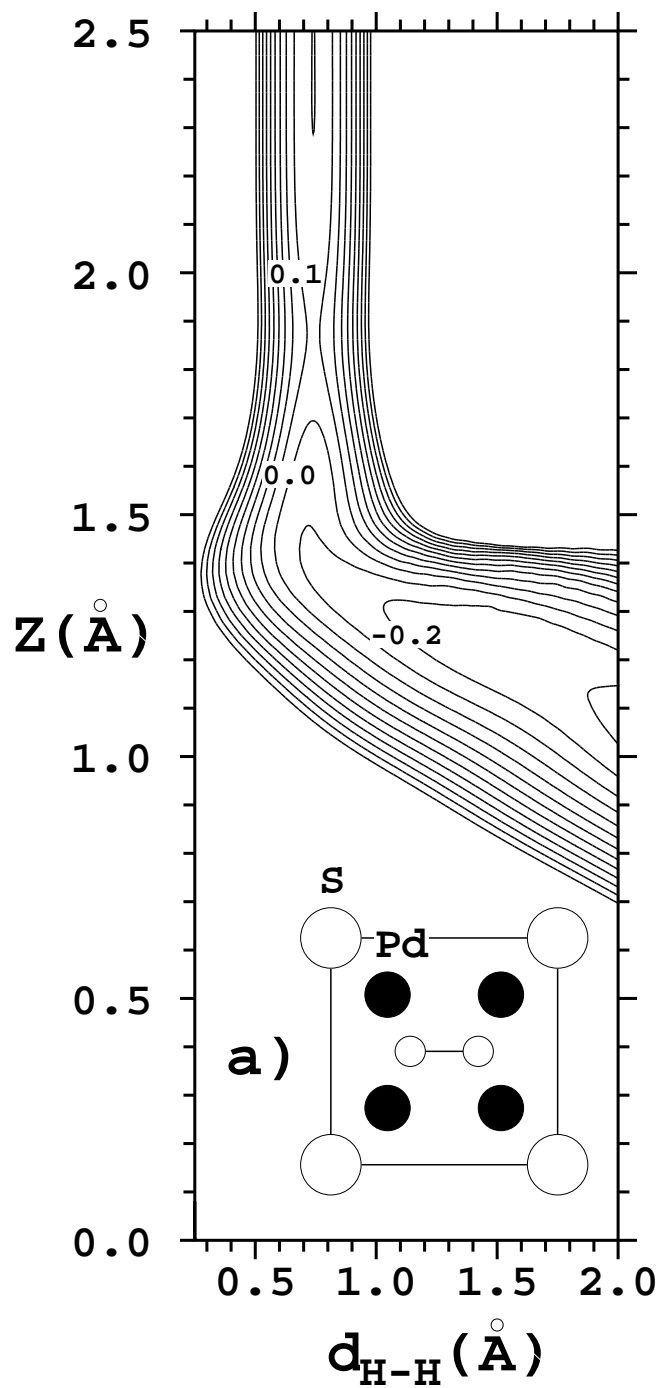


Fig. 14